Metal-Ion-Complexing Properties of 2-(Pyrid-2′-yl)-1, 10-phenanthroline, a More Preorganized Analogue of Terpyridyl. A Crystallographic, Fluorescence, and Thermodynamic Study

Ashley N. Carolan,[†] Amy E. Mroz,[†] Maya El Ojaimi,[‡] Donald G. VanDerveer,[§] Randolph P. Thummel,*[,‡] and Robert D. Hancock*[,†]

[†]Department of Chemistry and Biochemistry, University of North Carolina at Wilmington, Wilmington, North Carolina 28403, United States

[‡]Department of Chemistry, University of Houston, Houston, Texas 77004, United States

[§]Department of Chemistry, Clemson University, Clemson, South Carolina 29634, United States

Ⓢ *Supporting Information*

ABSTRACT: Some metal-ion-complexing properties of the ligand 2-(pyrid-2′-yl)-1,10-phenanthroline (MPP) are reported. MPP is of interest in that it is a more preorganized version of 2,2′;6,2″-terpyridine (tpy). Protonation constants ($pK_1 = 4.60$; $pK_2 = 3.35$) for MPP were determined by monitoring the intense $\pi - \pi^*$ transitions of 2×10^{-5} M solutions of the ligand as a function of the pH at an ionic strength of 0 and 25 °C. Formation constants ($\log K_1$) at an ionic strength of 0 and 25 °C were obtained by monitoring the $\pi - \pi^*$ transitions of MPP titrated with solutions of the metal ion, or 1:1 solutions of MPP and the metal ion were

titrated with acid. Large metal ions such as Ca^{II} or La^{III} showed increases of $\log K_1$ of about 1.5 log units compared to that of tpy. Small metal ions such as Zn^{II} and Ni^{II} showed little increase in $\log K_1$ for MPP compared to the tpy complexes, which is attributed to the presence of five-membered chelate rings in the MPP complexes, which favor large metal ions. The structure of $[Cd(MPP)(H_2O)(NO_3)_2]$ (**1**) is reported: monoclinic, $P2_1/c$, $a = 7.4940(13)$ Å, $b = 12.165(2)$ Å, $c = 20.557(4)$ Å, $\beta = 96.271(7)°$, $V = 1864.67(9)$ Å³, $Z = 4$, and final $R = 0.0786$. The Cd in **1** is seven-coordinate, comprising the three donor atoms of MPP, a coordinated water, a monodentate, and a bidentate NO_3^-. Cd^{II} is a fairly large metal ion, with $r^+ = 0.96$ Å, slightly too small for coordination with MPP. The effect of this size matching in terms of the structure is discussed. Fluorescence spectra of 2×10^{-7} M MPP in aqueous solution are reported. The nonprotonated MPP ligand fluoresces only weakly, which is attributed to a photoinduced-electron-transfer effect. The chelation-enhanced-fluorescence (CHEF) effect induced by some metal ions is presented, and the trend of the CHEF effect, which is $Ca^{II} > Zn^{II} > Cd^{II} \sim La^{III} > Hg^{II}$, is discussed in terms of factors that control the CHEF effect, such as the heavy-atom effect.

■ INTRODUCTION

The design of ligands for selective coordination of one metal ion over another in aqueous solution is important in a variety of applications:[1] sequestering of Cu^{II} and Zn^{II} in the brain, where they have been implicated in the occurrence of Alzheimer's disease;[2,3] sequestering Fe^{III}, which is suspected of being involved in Parkinson's disease;[4,5] selective removal of toxic metal ions such as Pb^{II} and Hg^{II} from the body in cases of metal intoxication;[6] complexes of Gd^{III} that are resistant to metal-ion substitution by Zn^{II} in the development of magnetic resonance imaging contrast agents;[7−13] selective removal of Am^{III} and Cm^{III} from mixtures of Ln^{III} ions (Ln = lanthanide) in the treatment of nuclear waste.[14,15] Metal-ion selectivity in solution is quantified by the difference in $\log K_1$ between metal ions of interest and the ligand being considered.[1] Guides in ligand design include Pearson's hard and soft acid and base principle[16−18] and features of the ligand architecture such as the chelate ring size,[1] where five-membered chelate rings are selective for large metal ions and six-membered chelate rings

are selective for small metal ions. Ligand preorganization[19] is also an important factor in ligand design. A preorganized ligand is one that has as its lowest energy conformation, or one of the lowest energy conformations, the conformation required to complex a target metal ion.[19] Appropriate preorganization gives complexes of greater thermodynamic stability and greater selectivity for target metal ions. Examples of preorganized ligands include crown ethers,[20] cryptands,[21] and aza-crowns.[22] One approach to a family of preorganized ligands has been to fuse a benzo ring to the halves of 2,2′-bipyridine (bpy) to create the more organized phenanthroline (phen) ligand[1,23,24] (see Figure 1 for ligand abbreviations). This organizational approach has led to ligands based on phen[24−26] such as PDA,[27−31] PDALC,[32,33] DPP,[34] PDAM,[35,36] and DPA,[37] as well as macrocyclic ligands such as L1 in Figure 1.[38−45]

Figure 1. Ligands discussed in this paper.

Ca^{2+} or La^{3+}, with ionic radii in the vicinity[46] of 1.0 Å, log K_1 is larger[37] than for the corresponding tpy complex[38] by about 3 log units, or roughly twice as much as that for the phen/bpy comparison. This comparison leads to the idea that making polypyridyl ligands more preorganized by the insertion of benzo groups into the ligand backbone will increase log K_1 by about 1.4 log units per benzo group addition. We report here a study of the metal-ion-complexing properties of 2-(pyrid-2'-yl)-1,10-phenanthroline (MPP) using fluorescence and UV–visible spectroscopy, as well as the structure of its complex with Cd^{II}. The interest in these polypyridyl ligands is the systematic way in which log K_1 increases with increasing numbers of pyridyl groups and reinforcing benzo groups, as illustrated for the La^{III} complexes, as summarized in Scheme 1.

Our interest here is whether one can develop a systematic approach to the design of reinforced polypyridyl ligands, including estimates of the complex stabilities and metal-ion selectivities of ligands of higher denticity and higher levels of preorganization such as diphen, L2, and DPPY in Figure 1. For example, one would estimate from the trends in Scheme 1 that, for example, DPPY would form a complex with La^{III} with the high log K_1 value for a purely N-donor ligand complexing a Ln^{III} ion of about 8.3.

A further point to be investigated is the fluorescence properties of MPP. DPP is of considerable significance in relation to its high selectivity for Cd^{II} over Zn^{II} as a fluorescent sensor.[34] This derives from both the much larger log K_1 of DPP with Cd^{II} than is the case for Zn^{II} and also the high chelation-enhanced-fluorescence (CHEF) effect displayed by Cd^{II} with DPP compared to the near-absence of any fluorescence of the Zn^{II}DPP complex. The lack of fluorescence with Zn^{II} is of importance in the design of sensors for Cd^{II}. Normally, Zn^{II} complexes fluoresce more strongly than Cd^{II} analogues, which

It has been noted that phen is more preorganized than bpy, so that log K_1 for phen complexes is a roughly constant 1.4 log units higher than that for the corresponding bpy complexes.[1] The ligand DPA[37] has shown interesting effects of preorganization compared to its less organized analogue 2,2';6,2"-terpyridine (tpy). In the case of DPA, for large metal ions such as

Scheme 1. Series of Ligands Showing How Increased Preorganization Provided by Reinforcing Benzo Groups, and an Increasing Number of Pyridyl Donor Groups, Affects log K_1 for Complexes of the Large Metal Ion La^{IIIa}
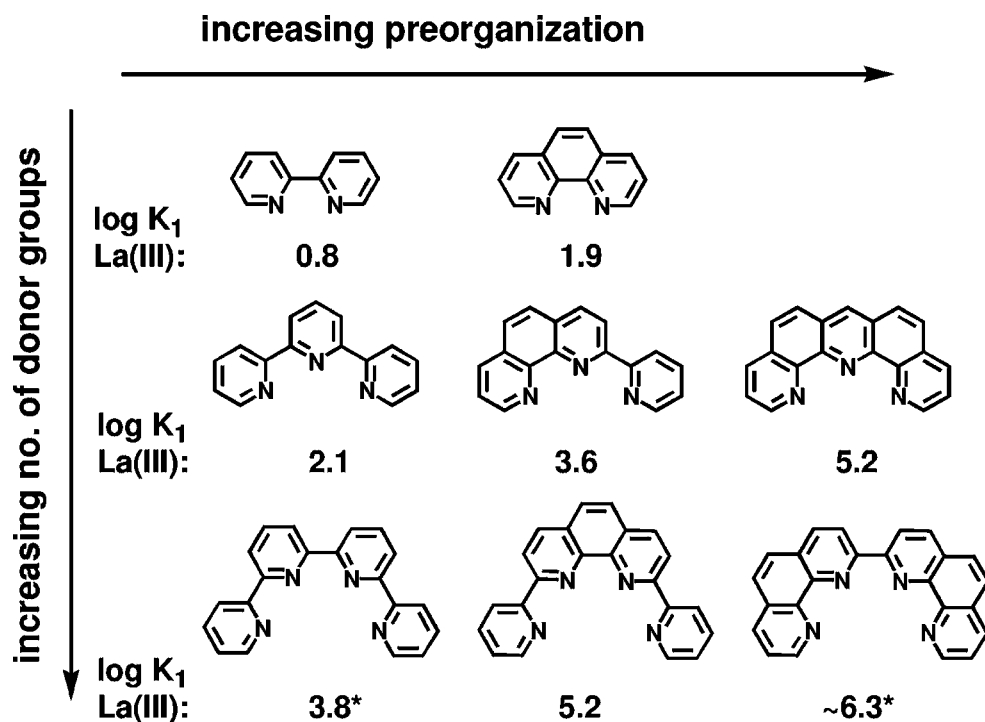
^{a}log K_1 data (this work) and refs 33 and 47−50. The asterisk indicates 50% MeOH.

is thought to be due to the larger spin−orbit coupling constants (ζ) associated with Cd^{II}. Where steric effects preclude Zn^{II} from coordinating sufficiently strongly with all of the lone pairs responsible for quenching the fluorescence of the free ligand (in the case of DPP, this is possibly the pyridyl N atoms), then no CHEF effect, or a greatly weakened CHEF effect, is observed.

■ EXPERIMENTAL SECTION

Materials and Methods. 2-(Pyrid-2′-yl)-1,10-phenanthroline (MPP) was synthesized by a published method.[50] The metal perchlorates were obtained from VWR or Strem in 99% purity or better and used as received. All solutions were made up in deionized water (Milli-Q, Waters Corp.) of >18 MΩ·cm^{-1} resistivity.

Synthesis of [Cd(MPP)H$_2$O(NO$_3$)$_2$] (1). A 1:1 solution of Cd^{II}MPP was prepared as follows: A total of 0.15 g of MPP was dissolved in 25 mL of acetone. In another beaker, 0.09 g of Cd(NO$_3$)$_2$·6H$_2$O was dissolved in 25 mL of ethanol and stirred. The solutions were combined and allowed to stand for 24 h. Colorless crystals of **1** were deposited and analyzed as follows. Calcd for C$_{17}$H$_{13}$CdN$_5$O$_7$: C, 39.90; H, 2.56; N, 13.69. Obsd: C, 39.70; H, 2.86; N, 13.92.

Molecular Structure Determination. A mounted crystal of **1** was placed in a cold nitrogen stream maintained at 168 K. A Rigaku AFC8S diffractometer with a 1K Mercury CCD detector was employed for crystal screening, unit cell determination, and data collection. The structures were solved by Patterson synthesis and refined to convergence.[51] Details of the structure determination of **1** are shown in Table 1, and these together with the crystal coordinates have been

Table 1. Crystal Data and Structure Refinement for 1

empirical formula	C$_{17}$H$_{13}$CdN$_5$O$_7$
fw	511.72
temperature (K)	168(2)
wavelength (Å)	0.710 73
cryst syst	monoclinic
space group	$P2_1/c$
unit cell dimens	$a = 7.4940(13)$
	$b = 12.165(2)$
	$c = 20.577(4)$
	$\beta = 96.271(7)$
volume (Å^3)	1864.67
Z	4
final R indices [$I > 2\sigma(I)$]	0.0786
R indices (all data)	0.1233

deposited with the Cambridge Structural Database (CSD).[52] Some more important bond lengths and angles for **1** are given in Table 2. The structure of **1** is shown in Figure 2.

Table 2. Bond Lengths and Angles of Interest in Complex 1

Bond Lengths (Å)					
Cd−N(1)	2.388(8)	Cd−N(14)	2.327(11)	Cd−N(20)	2.373(11)
Cd−O(1)	2.442(10)	Cd−O(2)	2.438(9)	Cd−O(4)	2.304(8)
Cd−O(7)	2.311(8)				

Bond Angles (deg)			
N(1)−Cd−N(14)	69.5(3)	N(14)−Cd−N(20)	69.1(4)
O(1)−Cd−O(2)	52.4(3)	Cd−O(4)−N(3)	118.3(3)
Cd−N(1)−C(10)	116.5(7)	Cd−N(14)−C(9)	119.3(8)
Cd−N(20)−C(15)	116.7(9)	Cd−N(14)−C(13)	116.9(10)

Formation Constant Studies. Protonation and formation constants in aqueous solution with a variety of metal ions were determined for MPP by monitoring the intense $\pi \rightarrow \pi^*$ transitions present in the UV spectrum. UV−visible spectra were recorded using a Varian 300 Cary 1E UV−visible spectrophotometer controlled by
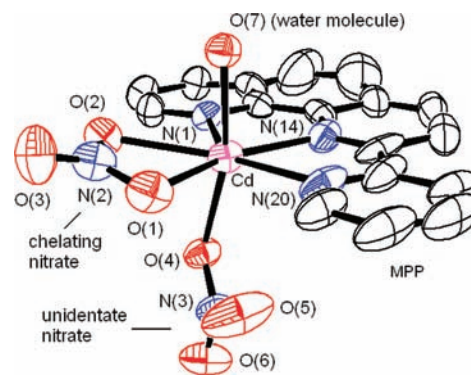
Figure 2. Structure of **1** showing the numbering scheme for atoms involved in the coordination sphere of the Cd. H atoms were omitted for clarity. Thermal ellipsoids were drawn at the 50% confidence level; the drawing was made with ORTEP.[55]

Cary Win UV Scan Application version 02.00(5) software. A VWR sympHony SR60IC pH meter with a VWR sympHony gel epoxy semimicro combination pH electrode was used for all pH measurements, which were made in the external titration cell, with N$_2$ bubbled through the cell to exclude CO$_2$. The pH meter was calibrated prior to each titration, by titration of standard acid with standard base. The value of $E°$ for the cell, as well as the Nernstian slope, was obtained from a linear plot of measured values of E versus the calculated pH. The jacketed cell containing 50 mL of a ligand/metal solution was thermostatted to 25.0 ± 0.1 °C.

As was found for DPA[37] and tpy,[47] the preparation of aqueous solutions of MPP initially proved problematic. It was found that the neutral form of MPP was more soluble in water than the protonated forms, especially the diprotonated form. A successful approach involved the preparation of a 10^{-3} M stock solution of MPP in MeOH (methanol) and then use of this solution to prepare 10^{-5} M aqueous solutions of MPP at neutral pH. Such solutions were stable and did not contain light-scattering peaks due to suspended particles.

In previous studies of complexes of phen-based ligands, a peristaltic pump was used to circulate a solution of the complex through a 1.0 cm quartz flow cell situated in the spectrophotometer.[27−36] As was the case with DPA,[37] it was found that, upon circulation of solutions of MPP complexes in this manner, the peak intensity steadily decreased with time, suggesting that MPP was being absorbed by the Tygon tubing used to connect the external cell with the flow cell in the spectrophotometer. The titrations were, therefore, carried out in an external jacketed cell, as described previously.[37] During the course of the titration, the cell was not moved because movement of the cell in the spectrophotometer causes irreproducible spectra.[53] As with DPA and tpy, it was also found that the addition of salts such as 0.1 M NaClO$_4$ to control the ionic strength (μ) resulted in solubility problems with MPP. Thus, the titrations were carried out with no added electrolyte, apart from the small amounts of acid or base added to adjust the pH and the small amounts of metal ions added to complex MPP. One thus sees in Figure 3a the series of three peaks that are thought to correspond to the LH$_2^{2+}$ (306 nm), LH$^+$ (303 nm), and free L (290 nm) (L = MPP). The set of spectra so obtained can be analyzed to yield two protonation constants pK_1 = 4.60(3) and pK_2 = 3.35(3) at μ = 0. The theoretical absorbance curves versus pH (Figure 3b) at several wavelengths were calculated using EXCEL.[54]

The formation constants for MPP complexes of Ca^{II}, La^{III}, Pr^{III}, Sm^{III}, Gd^{III}, Dy^{III}, Er^{III}, and Lu^{III} were determined by titrating an approximately neutral solution of MPP with 0.1 M solutions of the metal ion of interest, with no added electrolyte to control the ionic strength, as described previously.[37] The sets of spectra for the titration of 10^5 M MPP with Ca(ClO$_4$)$_2$ and Lu(ClO$_4$)$_3$ are seen in Figures 4 and 5. For Zn^{II}, Cd^{II}, and Pb^{II}, the log K_1 values were too high to be determined by titration of MPP with the metal ion, and for these complexes, a 1:1 solution of 10^{-5} M MPP and the metal perchlorate
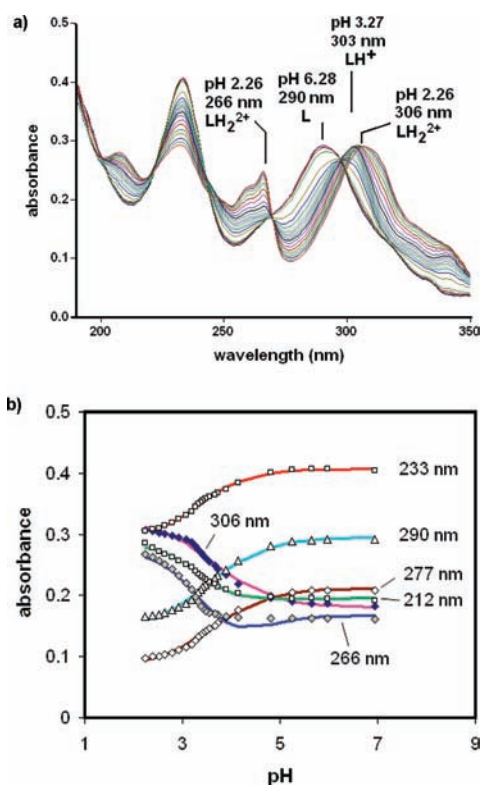
Figure 3. (a) Absorption spectra of an aqueous solution of 10^{-5} M MPP at 25.0 °C in the pH range 2.26−6.28. The peaks at 306 and 266 nm are assigned to the LH_2^{2+} species, while those at 303 and 290 nm are assigned to the LH^+ and L species, respectively (L = MPP). (b) Variation of the absorbance with the pH for 10^{-5} M MPP at 25 °C. The points represent the experimental values, while the solid lines are theoretical curves calculated using *SOLVER*[54] and protonation constants $pK_1 = 4.60$ and $pK_2 = 3.33$.
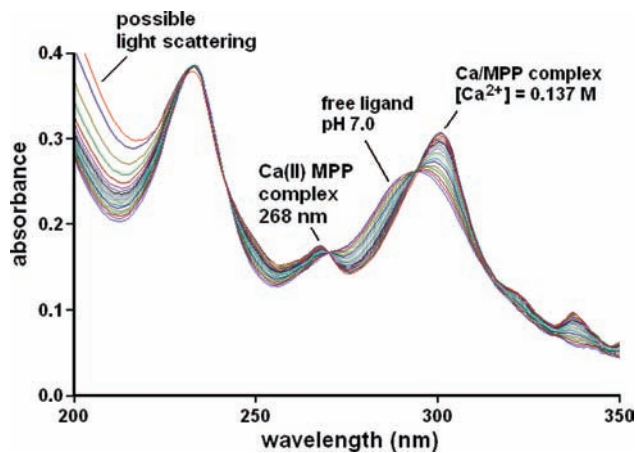
Figure 4. Absorption spectra in an aqueous solution of 10^{-5} M MPP at pH 6.2 titrated with a $Ca(ClO_4)_2$ solution, at 25 °C.

was titrated with $HClO_4$. One is then determining the equilibrium quotient (Q) for

$$M(MPP)^{2+} + 2H^+ \leftrightarrows MPPH_2^{2+} + M^{2+} \qquad (1)$$
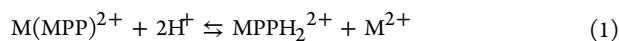
The protonation constants for MPP are thus combined with Q to give log K_1 for the MPP complexes. The spectra for the Zn[II]MPP titration are seen in Figure 6.

Theoretical absorbance curves versus the metal-ion concentration for metal/DPA titrations with Mg[II], Ca[II], Sr[II], Ba[II], and La[III], or of
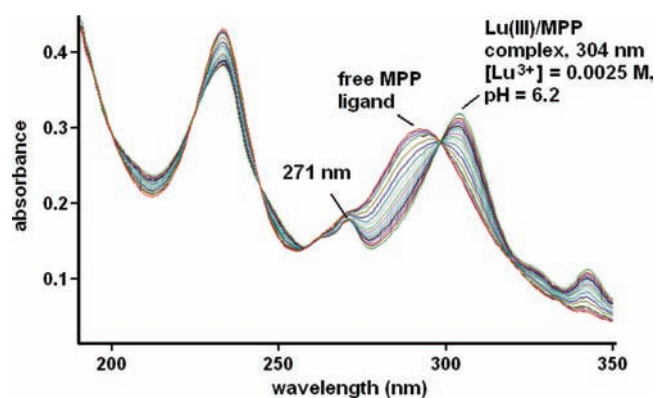
Figure 5. Absorption spectra in an aqueous solution of 10^{-5} M MPP at pH 6.2 titrated with a $Lu(ClO_4)_3$ solution, at 25 °C.
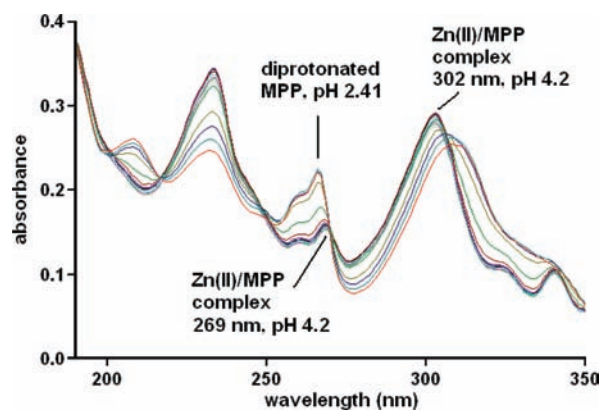
Figure 6. Absorption spectra in an aqueous solution of 10^{-5} M MPP and 10^{-5} M $Zn(ClO_4)_2$ between pH 2.41 and 4.2.

absorbance versus pH for the pK determinations plus titrations with Zn[II] and Cd[II], were fitted to the experimental data using the *SOLVER* function of *EXCEL*.[54] The standard deviations in the pK values given in Table 3 were calculated using the *SOLVSTAT* macro provided in ref 54.

Fluorescence Measurements. Excitation−emission matrix (EEM) fluorescence properties were determined on a Jobin-Yvon SPEX Fluoromax-3 scanning fluorometer equipped with a 150 W xenon arc lamp and a R928P detector. The instrument was configured to collect the signal in ratio mode with dark offset using 5 nm bandpasses on both the excitation and emission monochromators. The EEMs were created by concatenating emission spectra measured every 5 nm from 250 to 500 nm at 51 separate excitation wavelengths. Scans were corrected for instrument configuration using factory-supplied correction factors. Postprocessing of the scans was performed using the *FluorEssence* program.[56] The software eliminates Rayleigh and Raman scattering peaks by excising portions (±10−15 nm FW) of each scan centered on the respective scatter peak. The excised data are replaced using three-dimensional interpolation of the remaining data according to the Delaunay triangulation method and constraining the interpolation such that all nonexcised data are retained. Following removal of the scatter peaks, data were normalized to a daily determined water Raman intensity (275 ex/303 em; 5 nm bandpasses). Replicate scans were generally within 5% agreement in terms of the intensity and within bandpass resolution in terms of the peak location. The fluorescence of 2×10^{-7} M MPP solutions and solutions of MPP complexes with metal ions was recorded in aqueous solution, prepared in a manner similar to that in the absorbance studies from a 10^{-3} M stock solution of MPP in MeOH.

■ **RESULTS AND DISCUSSION**

Formation Constants. The formation constants determined here for MPP complexes are shown in Table 3.

Table 3. Protonation and Formation Constants for MPP Complexes in Aqueous Solution at 25 °C and an Ionic Strength of 0

Lewis acid	equilibrium	log K
H$^+$	H$^+$ + OH$^-$ ⇆ H$_2$O	13.997[a]
	H$^+$ + MPP ⇆ MPPH$^+$	4.60(3)
	MPPH$^+$ + H$^+$ ⇆ MPPH$_2$$^{2+}$	3.35(3)
Ca^{2+}	Ca^{2+} + MPP ⇆ Ca(MPP)$^{2+}$	2.24(5)
Ni^{2+}	Ni^{2+} + MPP ⇆ Ni(MPP)$^{2+}$	8.4(1)
Zn^{2+}	Zn^{2+} + MPP ⇆ Zn(MPP)$^{2+}$	7.8(1)
Cd^{2+}	Cd^{2+} + MPP ⇆ Cd(MPP)$^{2+}$	7.08(5)
Pb^{2+}	Pb^{2+} + MPP ⇆ Pb(MPP)$^{2+}$	7.15(5)
La^{3+}	La^{3+} + MPP ⇆ La(MPP)$^{3+}$	3.6(1)
Pr^{3+}	Pr^{3+} + MPP ⇆ Pr(MPP)$^{3+}$	4.12(5)
Sm^{3+}	Sm^{3+} + MPP ⇆ Sm(MPP)$^{3+}$	4.62(5)
Gd^{3+}	Gd^{3+} + MPP ⇆ Gd(MPP)$^{3+}$	4.4(1)
Dy^{3+}	Dy^{3+} + MPP ⇆ Dy(MPP)$^{3+}$	4.55(1)
Er^{3+}	Er^{3+} + MPP ⇆ Er(MPP)$^{3+}$	4.05(2)
Lu^{3+}	Lu^{3+} + MPP ⇆ Lu(DPA)$^{3+}$	4.57(2)

[a]Reference 49.

Dissolving ligands of low water solubility such as MPP in MeOH first and then using these MeOH solutions to make up aqueous solutions appear to work well, as is seen in the absorption spectra of MPP and its metal complexes in Figures 3a and 4−6. In all cases, good isosbestic points are obtained over the course of the titration, and light-scattering peaks appear to be absent, except for a small rise in the intensity near 200 nm in the titration of MPP with a Ca(ClO$_4$)$_2$ solution (Figure 4), which may be due to light scattering. The quantity of MPP particulates involved in such light scattering must be small because the isosbestic points continue to hold even at the higher Ca(ClO$_4$)$_2$ concentrations. As is customary in such cases, wavelengths below 250 nm were excluded in the determination of log K_1 for the Ca^{II}MPP complex because of possible interference with the absorbance values by light scattering. Omission of an electrolyte such as 0.1 M NaClO$_4$, normally added to control the ionic strength, appears to work well, and again no significant light-scattering peaks with absorbance >2.5 are observed. The same observation is made for ligands such as tpy, MPP, and DPA in higher ionic strength (μ) solutions.

In Table 4, the log K_1 values for the MPP and tpy[47] complexes of a selection of metal ions are shown, together with the ionic radii[46] of the metal ions. As has been found for ligands such as DPP and DPA, the presence of reinforcing benzo groups on the backbone of the ligand leads to stabilization of 1−2 log units for large metal ions such as La^{III} or Ca^{II} and virtually no stabilization for smaller metal ions such as Zn^{II}. It was found that there is a smaller increase in log K_1(MPP) for the large Pb^{II} ion compared with that of the tpy complex. This smaller increase is commonly encountered for metal ions with an ionic radius larger than the optimal radius of 1.0 Å and is found also for very large metal ions such as Ba^{II} with DPA.[37] The variation of log K_1 for the MPP and tpy complexes[47] of

Table 4. log K_1 Values (Ionic Strength = 0; 25 °C) of a Selection of Metal Ions with MPP (This Work) and tpy,[47] Together with Ionic Radii[46] for the Metal Ions

	metal ion						
	Zn^{II}	Cd^{II}	Ca^{II}	Pb^{II}	La^{III}	Gd^{III}	Lu^{III}
ionic radius (Å)[a]	0.72	0.96	1.00	1.19	1.03	0.94	0.86
log K_1(MPP)	7.8	7.1	2.2	7.2	3.6	4.4	4.6
log K_1(tpy)	7.6	6.3	0.9	6.0	2.1	2.6	2.8
Δ log K_1[b]	0.2	0.8	1.3	1.2	1.5	1.8	1.8

[a]Octahedral radii. [b]Δ log K_1 = log K_1(MPP) − log K_1(tpy).

some of the Ln^{III} ions as a function of the number of f electrons in the Ln^{III} ion is shown in Figure 7. The diagram shows a fairly
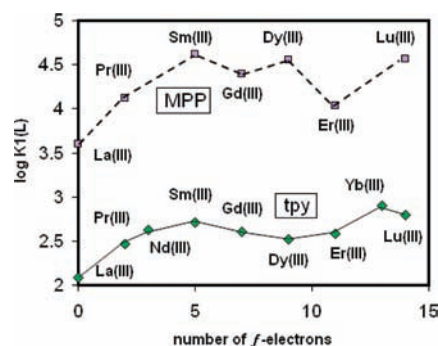
Figure 7. Variation of log K_1 for MPP and tpy complexes of Ln^{III} ions as a function of the number of f electrons in the Ln^{III} ion. Formation constant data: this work (MPP); ref 47 plus Carolan, A. N.; Hancock, R. D., to be published (tpy).

typical variation in log K_1 for the tpy complexes, with a modest rise in log K_1 from La^{III} to Lu^{III}. After Gd^{III}, there is a somewhat atypical drop in the complex stability before rising again to Lu^{III}. This variation may reflect the change in the coordination number observed[57] for the structures of Ln^{III}tpy complexes, where larger Ln^{III} ions such as La^{III} and Er^{III} formed nine-coordinate tpy complexes of the form [Ln(tpy)(H$_2$O)$_6$]$^{3+}$, while smaller Ln^{III} ions such as Tm^{III}, Yb^{III}, and Lu^{III} form eight-coordinate complexes of the type [Ln(tpy)(H$_2$O)$_5$]$^{3+}$. The small decline in log K_1 for the tpy complexes, culminating at Er^{III} (Figure 7), may reflect increasing steric crowding of the complex, relieved by the drop in the coordination number after Er^{III}, with a concomitant rise in log K_1 toward Lu^{III}. For the MPP complexes, the effects of steric crowding may parallel those of the tpy complexes, with a minimum in log K_1 at Er^{III}, but this effect may be exaggerated by the greater rigidity of the MPP ligand.

For all metal ions studied so far, there is a fairly steady rise in log K_1 as more pyridyl donors are added. Thus, for Zn^{II}, log K_1 varies: phen, 6.4; MPP, 7.8; DPP, 8.7. These increases in log K_1 can be attributed to (1) the affinity of metal ions for pyridyl donors, as indicated by log K_1 with pyridine itself and (2) the chelate effect,[58] where, from purely entropic considerations, one would expect an increase of log 55.5, or 1.74 log units, per donor group added,[1] arising from the asymmetry of the standard reference state.[59,60] Thus, a metal ion such as Cu^{II}, which has a larger log K_1(pyridine) of 2.5, shows large increases in log K_1 as more pyridyl donors are added, as seen in log K_1(bpy) = 8.12 and log K_1(tpy) = 12.3.[49] On the other hand, a metal ion such as Ca^{II}, which has a low affinity for pyridine, as indicated[49] by log K_1(pyridine) = −0.48, shows smaller

increases in log K_1 as pyridyl donors are added: K_1(bpy) = −0.1; log K_1(tpy) = 0.85; log K_1(qpy) = 2.52. In the case of Ca[II] and also La[III] in Scheme 1, the affinity of the metal ion for polypyridyl-type ligands would owe little to any inherent affinity for pyridyl donors, but the higher log K_1 values would be due almost entirely to preorganization by the chelate effect and preorganization of the ligand by reinforcing benzo groups.

Structural Studies. The structure of complex **1** is shown in Figure 2. Some bond lengths and angles of interest for **1** are given in Table 2. The Cd is seven-coordinate, and the complex is approximately pentagonal-bipyramidal, with the coordination sphere comprising the three donor atoms of the MPP ligand, a bidentate nitrate, a unidentate nitrate, and a coordinated water molecule. The average length for Cd−N bonds involving bpy- and phen-type complexes is 2.363 ± 0.03 Å (515 structures).[52] By this criterion, the two outer Cd−N bonds to MPP are slightly long at 2.382 Å, while the central Cd−N bond is slightly short at 2.327 Å. On the basis of molecular mechanics calculations, it has been suggested that the binding pocket provided by the donor atoms of the rigid DPA ligand causes metal ions that are too small to accommodate the curve formed by the ligand donor atoms to suffer exactly this type of bond-length distortion.[37] The central M−N bond to DPA, or in the present case MPP, will be compressed, while the outer M−N bonds will be stretched. The same effect is more marked for the DPP complex of Cd[II],[34] with the outer Cd−N bonds stretched to 2.559 Å and the inner Cd−N bonds compressed to 2.412 Å.

Of the approximately 7000 structures reported in the CSD[52] for Cd[II] complexes, six-coordination is greatly preferred (60.5%), followed by seven-coordination (16.9%), four-coordination (12.5%), five-coordination (7.4%), and eight-coordination (2.7%). In many cases, seven-coordination for complexes of Cd[II] appears to be promoted by ligands such as chelating nitrates or carboxylates, which have small bite distances, the O−O distances between the chelating O donors of the ligand. The higher coordination number of Cd observed in **1** thus may be promoted by the chelating nitrate present in the coordination sphere. A further factor may be that Cd[II] is slightly too small for optimal coordination with a polypyridyl ligand such as MPP. Coordination with DPA, which should be fairly similar to MPP, requires a best-fit M−N length of 2.60 Å,[37] compared with an average Cd−N bond length with polypyridyl-type ligands of 2.363 Å.[52] It may thus be that Cd[II] has also expanded its coordination number to move toward the geometric requirements of coordination with the MPP ligand.

Fluorescence Studies. The fluorescence of a 2×10^{-7} M MPP aqueous solution as a function of the pH, between pH 4.49 and 7.1, is shown in Figure 8. As was found for DPP,[34] the fluorescence of nonprotonated MPP at pH 7.1 is quite weak. It appears that a photoinduced-electron-transfer (PET) effect may be responsible for the weak fluorescence of nonprotonated MPP and DPP. In the PET effect, a lone pair on the ligand in the excited state transfers an electron into the gap in the π level of the fluorophore and thus hinders return of the excited-state electron to the ground state. The excited-state electron thus does not emit a photon and cause fluorescence. In the chelation-enhanced fluorescence (CHEF) effect, a metal ion binds to the lone pairs on the ligand and drops the energy of the lone pairs below that of the π level of the fluorophore, thus restoring fluorescence. This is summarized in Scheme 2.

In Figure 8, one sees that, as the pH drops from 7.1 to 4.49, there is a rise in the fluorescence intensity, a process similar to the CHEF effect, where the proton binds to the lone pair that
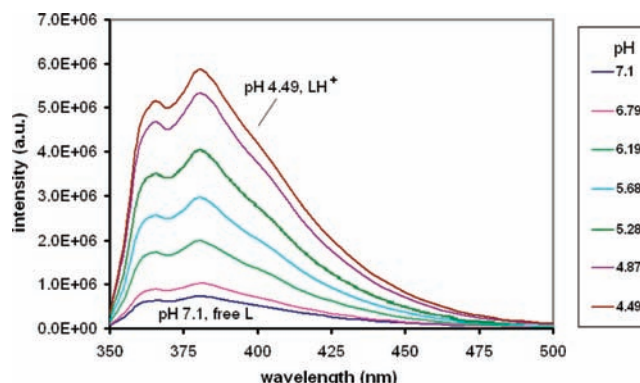
Figure 8. Fluorescence spectra of 2×10^{-7} M MPP in aqueous solution over a range of pH values from 4.49 to 7.1. Excitation wavelength = 300 nm.

quenches fluorescence by the PET effect (Scheme 2). At pH values below 4.49, there is a decrease in the fluorescence intensity (not shown) as the pH drops toward 2.0, and a second proton is added. Because the titration started at pH 7.1 with only 2×10^{-7} M MPP and no added electrolyte, this drop in the fluorescence intensity as the pH is lowered by the addition of HClO$_4$ may simply reflect collisional quenching[61] by the perchlorate anion. At pH values above 7.0, two additional protonation constants of 8.0 and 10.2 are indicated by variations in the fluorescence spectra. These higher protonation constants of aromatic amines, detectable from fluorescence, are considered to represent protonation of the excited state,[61,62] in this case of MPP. Thus, acridine has a pK_1 of 5.1 in the ground state, but its excited state has a pK_1* of 10.6.[61] (Excited-state constants are denoted by asterisks.) One sees here for MPP a similar pK_1* of 10.2 in the excited state, and also a pK_2* of 8.0.

In Figure 9 is shown the fluorescence of 2×10^{-7} M MPP as a function of the Ca^{2+} concentration. Ca^{2+} is normally excellent at producing a strong CHEF effect because it meets all of the requirements[63] for doing so. Factors that appear to affect the ability of a metal ion to produce a strong CHEF effect are as follows:[63] (1) *Large spin−orbit coupling constants* (ζ), which are present with heavy-metal ions such as Hg[II] or Pb[II]. These large ζ values facilitate intersystem crossing, which, in turn, produces longer-lived triplet states and so promotes radiationless paths to the ground state.[63] As seen in Figure 10, Hg[II] is quite effective at quenching the fluorescence of MPP. (2) *Paramagnetism.* Paramagnetic metal ions such as Cu[II], high-spin Ni[II], or Gd[III] strongly quench fluorescence. (3) Lighter metal ions such as Ca[II] and Zn[II] in Figure 10 that have smaller values of ζ are diamagnetic and are able to coordinate simultaneously to all of the fluorescence-quenching lone pairs on the ligand and produce the strongest CHEF effects. One notes the reasonably high fluorescence of the La[III] complex in Figure 10, in spite of La being a heavy atom, which therefore would be expected to have a large value of ζ. This high fluorescence intensity has been generally observed for the polypyridyl complexes of metal ions such as La[III] or Lu[III], and it appears that, in addition to the effects of a large value of ζ on the fluorescence intensity, a degree of covalence in the M−L bond may be necessary to communicate the effects of ζ to the fluorophore.[27] Ordinarily, Cd[II] with its somewhat larger value of ζ produces a smaller CHEF effect than does Zn[II]. However, ligands that sterically require a large metal ion with an ionic radius (r^+) close to 1.0 Å for effective overlap of the lone pairs on the ligand with the

Scheme 2. Origin of the PET and CHEF Effects in the Excited States of Fluorophores: (a) Fluorescence Quenched by the PET Effect; (b) Fluorescence Restored by the CHEF Effect
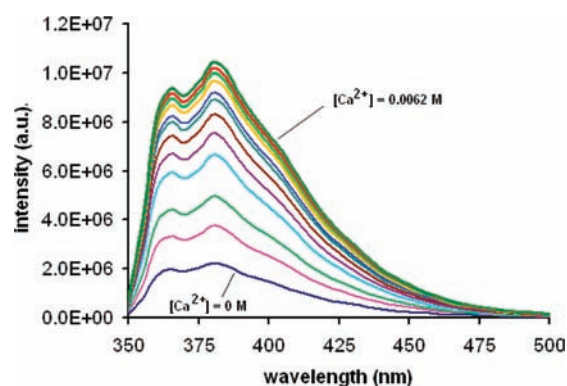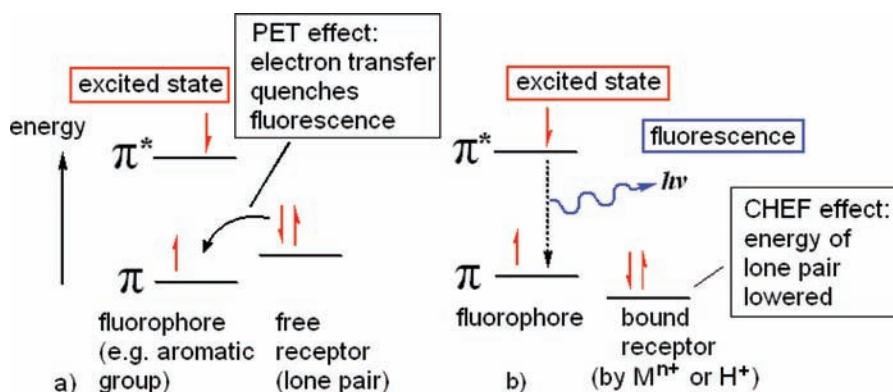
Figure 9. Fluorescence spectra in aqueous solution at pH 6.4 of 2×10^{-7} M MPP over a range of $Ca(ClO_4)_2$ concentrations from $[Ca^{2+}] = 0$ to 0.0062 M. Excitation wavelength = 300 nm.
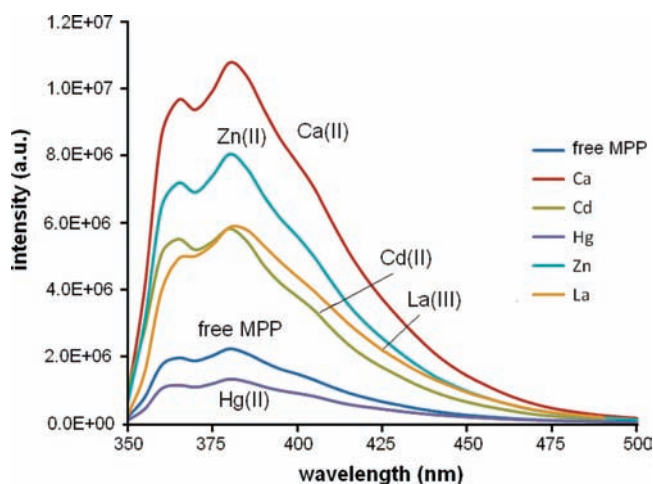
Figure 10. Fluorescence spectra in aqueous solution at pH 7.0 of MPP and some of its metal complexes, all with MPP = 2×10^{-7} M. All spectra of the MPP complexes were recorded with 1:1 MPP/metal ion ratios, except for Ca^{II}, which was 0.0062 M to ensure complete formation of the complex.

orbitals of the metal ion, as appears to be the case with DPP,[34] show a stronger CHEF effect with Cd^{II} than with Zn^{II}. One can get an idea of the Zn−N bond distortion that would be present in the DPP complex of Zn^{II} from the qpy complex of Zn^{II}.[64] Because Zn^{II} is too small ($r^+ = 0.74$ Å[46]) for qpy, which forms five-membered chelate rings and so requires a metal ion with

$r^+ \sim 1.00$,[1] one sees a N−Zn−N bond angle involving the outer N donors of qpy of 135.7° instead of the 90° expected for an octahedron and Zn−N bonds to these outer N donors of 2.181 Å compared to the more normal Zn−N bonds to the inner pair of N donors of 2.119 Å. The diminished overlap with the lone pairs of the N donors of DPP would lead to a diminished CHEF effect. MPP is not nearly so sterically demanding a ligand as DPP, so that a fairly normal pattern of the CHEF effect of Zn^{II} > Cd^{II} is observed in Figure 10, although even with MPP, Cd^{II} is much closer in fluorescence intensity to Zn^{II} than usual.

It was found that the fluorescence of the Ca^{II}MPP complex in Figure 9 suggests that complex formation is complete at a Ca^{II} concentration of only 0.0062 M, but the fact that the log K_1(MPP) value of 2.24 reported here would suggest that the complex would only be some 50% formed at such a Ca^{II} concentration. This is a phenomenon that we have encountered more than once in the study of polypyridyl complexes, which suggests that one cannot use fluorescence for the reliable determination of log K_1 in these instances. We are attempting to understand this phenomenon, and our current thinking is that it relates to the fact that fluorescence originates from the excited state of the complex, and just as aromatic amines have protonation constants of the excited state that are higher than those of the ground state,[61,62] so the stability of the excited-state complex of Ca^{II} here appears to be higher than that of the ground state.

■ **CONCLUSIONS**

The log K_1 results for MPP, and those indicated in Scheme 1, suggest a fairly predictable pattern of behavior, where large metal ions such as Ca^{II} or La^{III} show an approximately 1.5 log unit increase in log K_1 per added reinforcing benzo group, while small metal ions such as Zn^{II} or Mg^{II} do not, and the addition of extra coordinating pyridyls along a series such as bpy, tpy, and qpy or phen, MPP, and DPP produces a steady increase in log K_1, with the increase dependent on the affinity of the metal ion for pyridyl N donors. One should thus be able to predict the stabilities of even more complex ligands such that log K_1 for La^{III} with triphen in Figure 1 would be as high as 15. The fluorescence properties of MPP are as expected from considering what metal-ion properties influence their ability to produce the CHEF effect. The order of the strength of the CHEF effect for MPP complexes is Ca^{II} > Zn^{II} > Cd^{II} ~ La^{III} ≫ Hg^{II}, which is also the order of increasing spin−orbit coupling constants, which leads to increasing quenching of fluorescence.

■ ASSOCIATED CONTENT

S Supporting Information

X-ray crystallographic data in CIF format. This material is available free of charge via the Internet at http://pubs.acs.org.

■ AUTHOR INFORMATION

Corresponding Author

*E-mail: thummel@uh.edu (R.P.T.), hancockr@uncw.edu (R.D.H.).

Notes

The authors declare no competing financial interest.

■ ACKNOWLEDGMENTS

■ REFERENCES

(1) Hancock, R. D.; Martell, A. E. *Chem. Rev.* **1989**, *89*, 1875.

(2) Barnham, K. J.; Bush, A. I. *Curr. Opin. Chem. Biol.* **2008**, *12*, 222.

(3) Maynard, C. J.; Bush, A. I.; Masters, C. L.; Cappai, R.; Li, Q.-X. *Int. J. Exp. Pathol.* **2005**, *86*, 147.

(4) Gerlach, M.; Double, K. L.; Youdim, M. B. H.; Riederer, P. *J. Neural Trans. Suppl.* **2006**, *70*, 133.

(5) Rhodes, S. L.; Ritz, B. *Neurobiol. Dis.* **2008**, *32*, 183.

(6) Andersen, O. *Chem. Rev.* **1999**, *99*, 2683.

(7) Aime, S.; Delli Castelli, D.; Geninatti Crich, S.; Gianolio, E.; Terreno, E. *Acc. Chem. Res.* **2009**, *42*, 822.

(8) Datta, A.; Raymond, K. N. *Acc. Chem. Res.* **2009**, *42*, 938.

(9) Caravan, P. *Acc. Chem. Res.* **2009**, *42*, 851.

(10) Sherry, A. D.; Woods, M. *Annu. Rev. Biomed. Eng.* **2008**, *10*, 391.

(11) Port, M.; Idee, J.-M.; Medina, C.; Robic, C.; Sabatou, M.; Corot, C. *BioMetals* **2008**, *21*, 469.

(12) Caravan, P.; Ellison, J. J.; McMurry, T. J.; Lauffer, R. B. *Chem. Rev.* **1999**, *99*, 2293.

(13) Maiocchi, A. *Mini-Rev. Med. Chem.* **2003**, *3*, 845.

(14) Nash, K. L.; Madic, C.; Mathur, J. N.; Lacquement, J. In *The chemistry of the actinide and transactinide elements*, 3rd ed.; Morss, L. R., Edelstein, N. M., Fuger, J., Eds.; Springer: Dordrecht, The Netherlands, 2006; Vol. 4, p 2622.

(15) Kolarik, Z. *Chem. Rev.* **2008**, *108*, 4208.

(16) Pearson, R. G.; Mawby, R. *J. Halogen Chem.* **1967**, *3*, 55.

(17) Pearson, R. G. *Coord. Chem. Rev.* **1990**, *100*, 403.

(18) Pearson, R. G. *Chemical Hardness*; Wiley-VCH: Weinheim, Germany, 1997.

(19) Cram, D. J.; Cram, J. M. *Acc. Chem. Res.* **1978**, *11*, 8.

(20) Pederson, C. J. *J. Am. Chem. Soc.* **1967**, *89*, 2495.

(21) Lehn, J. M. *Acc. Chem. Res.* **1978**, *11*, 49.

(22) Cabbiness, D. K.; Margerum, D. W. *J. Am. Chem. Soc.* **1969**, *91*, 6540.

(23) Accorsi, G.; Listorti, A.; Yoosaf, K.; Armaroli, N. *Chem. Soc. Rev.* **2009**, *38*, 1690.

(24) Bencini, A.; Lippolis, V. *Coord. Chem. Rev.* **2010**, *254*, 2096.

(25) Coates, J.; Sammes, P. G.; West, R. M. *J. Chem. Soc., Perkin Trans. 2* **1996**, *7*, 1275.

(26) Hancock, R. D.; Melton, D. L.; Harrington, J. M.; McDonald, F. C.; Gephart, R. T.; Boone, L. L.; Jones, S. B.; Dean, N. E.; Whitehead, J. R.; Cockrell, G. M. *Coord. Chem. Rev.* **2007**, *251*, 1678.

(27) Melton, D. L.; VanDerveer, D. G.; Hancock, R. D. *Inorg. Chem.* **2006**, *45*, 9306.

(28) Dean, N. E.; Hancock, R. D.; Cahill, C. L.; Frisch, M. *Inorg. Chem.* **2008**, *47*, 2000.

(29) Williams, N. J.; Dean, N. E.; VanDerveer, D. G.; Luckay, R. C.; Hancock, R. D. *Inorg. Chem.* **2009**, *48*, 7853.

(30) Moghimi, A.; Alizadeh, R.; Shokrollahi, A.; Aghabozorg, H.; Shamsipur, M.; Shockravi, A. *Inorg. Chem.* **2003**, *42*, 1616.

(31) Fan, L.-L.; Li, C.-J.; Meng, Z.-S.; Tong, M.-L. *Eur. J. Inorg. Chem.* **2008**, 3905.

(32) Gephart, R. T. III; Williams, N. J.; Reibenspies, J. H.; De Sousa, A. S.; Hancock, R. D. *Inorg. Chem.* **2008**, *47*, 10342.

(33) Gephart, R. T. III; Williams, N. J.; Reibenspies, J. H.; De Sousa, A. S.; Hancock, R. D. *Inorg. Chem.* **2009**, *48*, 8201.

(34) Cockrell, G. M.; Zhang, G.; VanDerveer, D. G.; Thummel, R. P.; Hancock, R. D. *J. Am. Chem. Soc.* **2008**, *130*, 1420.

(35) Merrill, D.; Hancock, R. D. *Radiochim. Acta* **2011**, *99*, 161.

(36) Merrill, D.; Harrington, J. M.; Lee, H.-S.; Hancock, R. D. *Inorg. Chem.* **2011**, *50*, 8348.

(37) Hamilton, J. M.; Whitehead, J. R.; Williams, N. J.; El Ojaimi, M.; Thummel, R. P.; Hancock, R. D. *Inorg. Chem.* **2011**, *50*, 3785.

(38) Bazzicalupi, C.; Bencini, A.; Fusi, V.; Giorgi, C.; Paoletti, P.; Valtancoli, B. *J. Chem. Soc., Dalton Trans.* **1999**, 393.

(39) Bazzicalupi, C.; Bencini, A.; Bianchi, A.; Giorgi, C.; Fusi, V.; Valtancoli, B.; Bernado, M. A.; Pina, F. *Inorg. Chem.* **1999**, *38*, 3806.

(40) Arca, M.; Blake, A. J.; Casabo, J.; Demartin, F.; Devillanova, F. A.; Garau, A.; Isaia, F.; Lippolis, V.; Kivekas, R.; Muns, V.; Schroder, M.; Verani, G. *J. Chem. Soc., Dalton Trans.* **2001**, 1180.

(41) Blake, A. J.; Devillanova, F. A.; Garau, A.; Harrison, A.; Isaia, F.; Lippolis, V.; Tiwary, S. K.; Schroder, M.; Verani, G.; Whittaker, G. *J. Chem. Soc., Dalton Trans.* **2002**, 4389.

(42) Arca, M.; Azimi, G.; Demartin, F.; Devillanova, F. A.; Escriche, L.; Garau, A.; Isaia, F.; Kivekas, R.; Lippolis, V.; Muns, V.; Perra, A.; Shamsipur, M.; Sportelli, L.; Yari, A. *Inorg. Chim. Acta* **2005**, *358*, 2403.

(43) Blake, A. J.; Casabo, J.; Devillanova, F. A.; Escriche, L.; Garau, A.; Isaia, F.; Lippolis, V.; Kivekas, R.; Muns, V.; Schroder, M.; Sillanpaa, R.; Verani, G. *J. Chem. Soc., Dalton Trans.* **1999**, 1085.

(44) Aragoni, M. C.; Arca, M.; Bencini, A.; Biagini, S.; Blake, A. J.; Caltagirone, C.; Demartin, F.; De Filippo, G.; Devillanova, F. A.; Garau, A.; Gloe, K.; Isaia, F.; Lippolis, V.; Valtancoli, B.; Wenzel, M. *Inorg. Chem.* **2008**, *47*, 8391.

(45) Bencini, A.; Berni, E.; Bianchi, A.; Fornasari, P.; Giorgi, C.; Lima, J. C.; Lodeiro, C.; Melo, M. J.; Seixas de Melo, J.; Parola, A. J.; Pina, F.; Pina, J.; Valtancoli, B. *Dalton Trans.* **2004**, 2180.

(46) Shannon, R. D. *Acta Crystallogr., Sect. A* **1976**, *A32*, 751.

(47) Hamilton, J. M.; Anhorn, M. J.; Oscarson, K. A.; Reibenspies, J. H.; Hancock, R. D. *Inorg. Chem.* **2011**, *50*, 2764.

(48) Hancock, R. D.; Jackson, J.; Evers, A. *J. Chem. Soc., Dalton Trans.* **1979**, 1384.

(49) Martell, A. E.; Smith, R. M. *Critical Stability Constant Database*; National Institute of Science and Technology (NIST): Gaithersburg, MD, 2003; Vol. 46.

(50) Hung, C.-Y.; Wang, T.-L.; Shi, Z.; Thummel, R. P. *Tetrahedron* **1994**, *50*, 10685.

(51) *SHELXTL*, version 6.10: Sheldrick, G. M. *Acta Crystallogr., Sect. A* **2008**, *A64*, 112.

(52) Allen, F. H. *Acta Crystallogr., Sect. B: Struct. Sci.* **2002**, *B58*, 380. Cambridge Structure Database, version 5.3, 2011.

(53) Skoog, D. A.; Holler, E. J.; Crouch, S. R. *Principles of Instrumental Analysis*; Thomson: Belmont, CA, 2007; pp 343−346.

(54) Billo, E. J. *EXCEL for Chemists*; Wiley-VCH: New York, 2001.

(55) *ORTEP-3 for Windows*, version 1.08: Farrugia, L. J. *J. Appl. Crystallogr.* **1997**, *30*, 565.

(56) *FluorEssence program*, version 2.1; Horiba Jobin Yvon, Inc.: Edison, NJ, 2006.

(57) Semenova, L. I.; White, A. H. *Aust. J. Chem.* **1999**, *52*, 539.

(58) Schwarzenbach, G. *Helv. Chim. Acta* **1952**, *35*, 2344.

(59) Adamson, A. W. *J. Am. Chem. Soc.* **1954**, *76*, 1578.

(60) Hancock, R. D.; Marsicano, F. *J. Chem. Soc., Dalton Trans.* **1976**, 1096.

(61) Lakowicz, J. R. *Principles of Fluorescence Spectroscopy*, 2nd ed.; Plenum: New York, 1999; pp 211 and 516.

3014

dx.doi.org/10.1021/ic202337v | *Inorg. Chem.* 2012, 51, 3007–3015

(62) Marciniak, B.; Kozubek, H.; Paszyc, S. *J. Chem. Educ.* **1992**, *69*, 247.

(63) de Silva, A. P.; Gunaratne, H. Q. N.; Gunnlaugsson, T.; Huxley, A. J. M.; McCoy, C. P.; Rademacher, J. T.; Rice, T. E. *Chem. Rev.* **1997**, *97*, 1515.

(64) Dell'Amico, D. B.; Calderazzo, F.; Curiardi, M.; Labella, L.; Marchetti, F. *Inorg. Chem.* **2004**, *43*, 5459.

3015

dx.doi.org/10.1021/ic202337v | *Inorg. Chem.* 2012, 51, 3007−3015